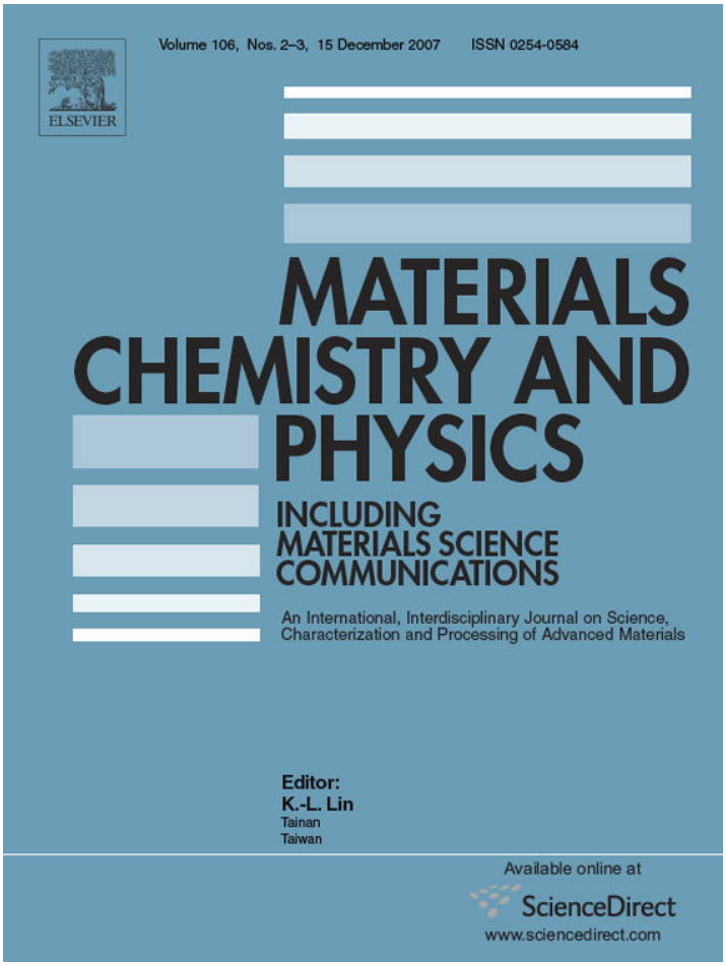

Available online at www.sciencedirect.com
ScienceDirect
Materials Chemistry and Physics 106 (2007) 168–174
MATERIALS CHEMISTRY AND PHYSICS
www.elsevier.com/locate/matchemphys

Tungsten trioxide nanorods as supports for platinum in methanol oxidation

Janarthanan Rajeswari, Balasubramanian Viswanathan *, Thirukkallam Kanthadai Varadarajan

National Centre for Catalysis Research, Department of Chemistry, Indian Institute of Technology Madras, Chennai 600036, India

Received 24 October 2006; received in revised form 28 April 2007; accepted 20 May 2007

Abstract

Tungsten trioxide (WO_3) nanorods have been prepared by a simple pyrolysis of surfactant encapsulated tungsten oxide clusters. These nanorods are characterized by XRD, Raman, electron microscopic techniques and cyclic voltammetry. Platinum nanoparticles have been supported on these WO_3 nanorods. The electrocatalytic activity and stability of platinum loaded WO_3 nanorods towards methanol oxidation have been studied and compared with that of platinum supported on bulk WO_3 and commercial 20% Pt-Ru/C (J.M.) using electrochemical measurements. The results demonstrated that alteration of the morphology of the WO_3 from bulk to 1D nanorods have resulted in comparable methanol oxidation activity as that of the commercial 20% Pt-Ru/C catalyst.

Keywords: Tungsten trioxides; Nanorods; Methanol oxidation; Electrochemical techniques

1. Introduction

Direct methanol fuel cells (DMFCs) have attracted considerable interest as potential power sources for stationary and transportation applications because of its system simplicity, low pollution and high efficiency [1–4]. Methanol as fuel in DMFC has several potential features. It is easily stored, transported, handled and has a high theoretical energy density. Because of these potential features, electro-oxidation of methanol has been extensively studied in the past decades [5–9]. However, the main draw back of the DMFC is insufficient activity of the platinum catalyst at the anode. Pure platinum is poisoned by reaction intermediates such as CO [10–15]. Before effective commercialization of DMFC, the problem of losses caused by excessive CO poisoning has to be solved. In order to overcome the drawbacks and to improve the catalyst performance, platinum based alloys (such as, Pt–Ru, Pt–Os, Pt–Sn) are used in DMFCs [16–19]. Pt–Ru supported on carbon is the most active catalyst for methanol oxidation. The enhancement of the catalytic activity of platinum in the presence of ruthenium was explained by various mechanisms [20–23]. Still, this system is not good enough for commercial applications due to its prohibitively high cost and limited supplies of Pt and Ru [24]. Metal–metal oxide catalysts are also being investigated for electro-oxidation reactions [25]. Specifically, tungsten oxide (WO_3) based catalysts have been studied by several groups as potential low-cost fuel cell catalysts [26–34]. The improvement in methanol oxidation activity in Pt-WO_3 catalysts is partly attributed to the ability of WO_3 to intercalate H atoms into its matrix, forming highly conductive tungsten bronzes. The dehydrogenation steps in the methanol oxidation reaction are thus facilitated, resulting in a higher turnover on Pt sites. Moreover, the OH_{ads} groups on WO_3 facilitates oxidation of CO intermediates [35–38]. A great deal of interest still exists in the development of materials capable of the electrocatalytic oxidation of methanol, in order to diminish the typically large overpotentials encountered in its direct oxidation at most electrode surfaces. Particular interest has been centered on materials that can be synthesized on nanometer scale with controlled nanostructures for achieving efficient catalysts for use in fuel cells [39,40]. The physical, electrochemical, electronic, and optical properties of nanostructured materials are well known to be different from those of bulk materials. Recently, one-dimensional (1D) nanorods have attracted remarkable attention owing to their unique properties and potential for various novel

* Corresponding author. Tel.: +91 44 2257 4241; fax: +91 44 2257 4202.
E-mail address: bvnathan@iitm.ac.in (B. Viswanathan).

0254-0584/$ – see front matter © 2007 Elsevier B.V. All rights reserved.
doi:10.1016/j.matchemphys.2007.05.032

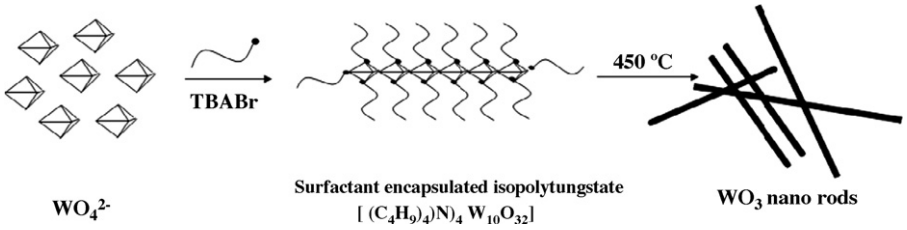

Scheme 1. Fabrication of WO_3 nanorods.

applications [41]. Nanorods have large specific surface areas; the decoration of Pt nanoparticles on the support of nanorods could efficiently prevent Pt nanoparticles from the agglomeration. Therefore, synthesis of 1D WO_3 nanorods would produce an efficient support for the catalyst with a synergetic effect of the properties of both nanorods as well as WO_3 for methanol oxidation. The aim of the current study is to verify such a supposition experimentally, which is of significant importance for the design of catalysts. Several synthetic approaches including thermal, electrochemical etching, template directed synthesis, wet chemical organic or inorganic routes have been applied to fabricate WO_3 nanorods [42–48]. We report a surfactant directed large-scale synthesis of single crystalline WO_3 nanorods formed by a simple, single step pyrolysis of surfactant encapsulated tungsten oxide clusters. The employed route is template free, contaminant free, easy, economical and requires a low temperature for the fabrication of WO_3 nanorods. The so-fabricated WO_3 nanorods were used as supports for platinum nanoparticles (Pt/WO_3 nanorods) in methanol oxidation and the catalytic activity of this system has been compared with that of commercially available Johnson Matthey carbon supported 20% Pt-Ru catalyst (Pt-Ru/C (J.M.)) and bulk WO_3 supported 20% Pt (Pt/bulk WO_3). Bulk WO_3 is commercially obtained from Alfa Aesar (A Johnson Matthey Company).

2. Experimental

2.1. Synthesis of WO_3 nanorods and loading of platinum on WO_3 nanorods

The precursor compound, tetrabutylammonium decatungstate $((C_4H_9)_4N)_4W_{10}O_{32}$ was synthesized as described elsewhere [49] by using $Na_2WO_4{\cdot}2H_2O$ and tetrabutylammonium bromide (TBABr) as the starting materials. The precursor was recrystallized in hot dimethyl formamide to give yellow crystals. The thermogravimetric analysis revealed that the cation content in the compound is 29.0% (calculated value: 29.2%). The pyrolysis of tetrabutylammonium decatungstate to synthesize WO_3 nanorods is carried out as follows: 1 g of the precursor was taken in an alumina or quartz boat and introduced inside a tubular furnace and heated at 450 °C at a heating rate of 25 °C per min under Ar atmosphere for 3 h. Then it was gradually cooled to room temperature to obtain a blue powder of WO_3 nanorods. The total yield of the obtained material was 71% by weight (relative to the starting material). To load 20% Pt on WO_3, wet impregnation method was adopted wherein 0.01 M aqueous hexachloroplatinic acid (H_2PtCl_6) was mixed with required amount of WO_3 nanorods by stirring at room temperature. It was then evaporated to dryness followed by reduction in hydrogen atmosphere at 350 °C for 4 h.

2.2. Characterization of WO_3 nanorods and Pt/WO_3 nanorods

X-ray diffraction (XRD) patterns were obtained by a powder diffractometer (XRD-SHIMADZU XD-D1) using a Ni-filtered Cu Kα X-ray radiation source. CRM 200 Raman spectrometer was employed, using the 514.5 nm line of an Ar ion laser as the excitation source. The morphology of the WO_3 nanorods and bulk WO_3 were investigated by a scanning electron microscopy (SEM) (FEI, Model: Quanta 200). Transmission electron microscopy (TEM), electron diffraction and energy dispersive X-ray analysis (EDAX) were performed on a Philips CM12/STEM instrument. High-resolution transmission electron microscopy (HRTEM) was carried out on a JEOL 3010 instrument to characterize the WO_3 nanorods and platinum loaded WO_3 nanorods.

2.3. Electrochemical measurements

Cyclic voltammetry and chronoamperometry were performed on a BAS Epsilon potentiostat. The measurements were made using a three electrode cell set up. An Ag/AgCl, saturated KCl electrode and a Pt foil were used as reference and counter electrodes, respectively. The working electrode was fabricated by dispersing the platinum-supported catalysts in distilled water. The dispersion was ultrasonicated for 15 min. A known amount of the dispersion was transferred onto a glassy carbon electrode and the water was evaporated slowly. The resulting film was covered with 5 μl of 5% Nafion solution in order to fix the particles on the substrate. A solution of 1 M CH_3OH in 1 M H_2SO_4 was used to study the methanol oxidation activity. All the electrochemical studies were performed at a scan rate of 25 mV s^{-1}.

3. Results and discussion

3.1. Mechanism for the formation of WO_3 nanorods

The mechanism for the formation of WO_3 nanorods is proposed as shown in Scheme 1: Na_2WO_4 and tetrabutylammonium bromide (TBABr) reacts to form the precursor compound $((C_4H_9)_4)N)_4W_{10}O_{32}$. In the precursor compound, inorganic metal oxide clusters ($W_{10}O_{32}{}^{4-}$) are charge balanced with the surfactant group (TBABr). TBABr restricts the irregular arrangement of the metal oxide clusters by providing a steric environment around them. This leads to the formation of 1D array of metal oxide clusters. During pyrolysis at 450 °C, removal of the surfactant species ($(C_4H_9)_4N^+$) and decomposition of the $W_{10}O_{32}$ leads to the formation of pure, single crystalline WO_3 nanorods.

3.2. Characterization of WO_3 nanorods and platinum loaded WO_3 nanorods

The XRD patterns of as received commercial tungsten trioxide (bulk WO_3) and as-synthesized tungsten oxide (WO_3 nanorods) have been shown in Fig. 1a and b, respectively. Both the diffraction patterns are well in agreement with the single crystalline monoclinic WO_3 (JCPDS card no. 75-2072). The XRD pattern of WO_3 nanorods reveal a predominant growth along the (0 2 0) plane. The XRD pattern of Pt loaded WO_3

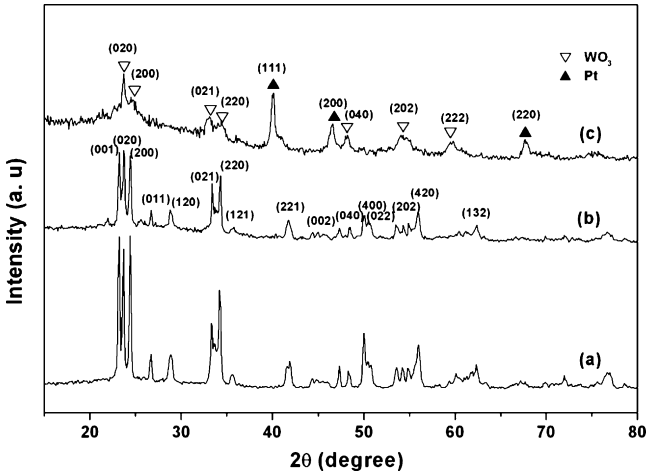

Fig. 1. XRD patterns of (a) bulk WO_3, (b) WO_3 nanorods, and (c) Pt/WO_3 nanorods.

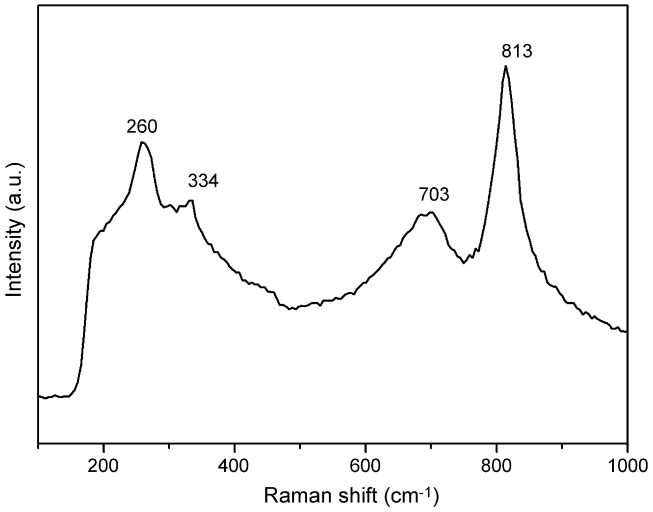

Fig. 2. Micro-Raman spectrum of WO_3 nanorods.

nanorods is given in Fig. 1c. The diffraction pattern corresponds to the reflections of monoclinic WO_3 nanorods and face centered cubic Pt (JCPDS card no. 04-0802).

The Raman spectrum shown in Fig. 2 indicates four bands at ~260, 334, 703 and 813 cm^{-1} which agree closely to the wave numbers of the strongest modes of monoclinic-WO_3. The bands at 260 and 334 cm^{-1} correspond to O–W–O bending modes and the bands at 703 and 813 cm^{-1} can be attributed to the stretching modes of the WO_3 [50–52].

SEM was employed to observe the morphology of the commercially obtained tungsten trioxide (Fig. 3a and b) and the as-synthesized WO_3 nanorods (Fig. 3c and d). The commercially obtained tungsten trioxide revealed agglomerated particles with

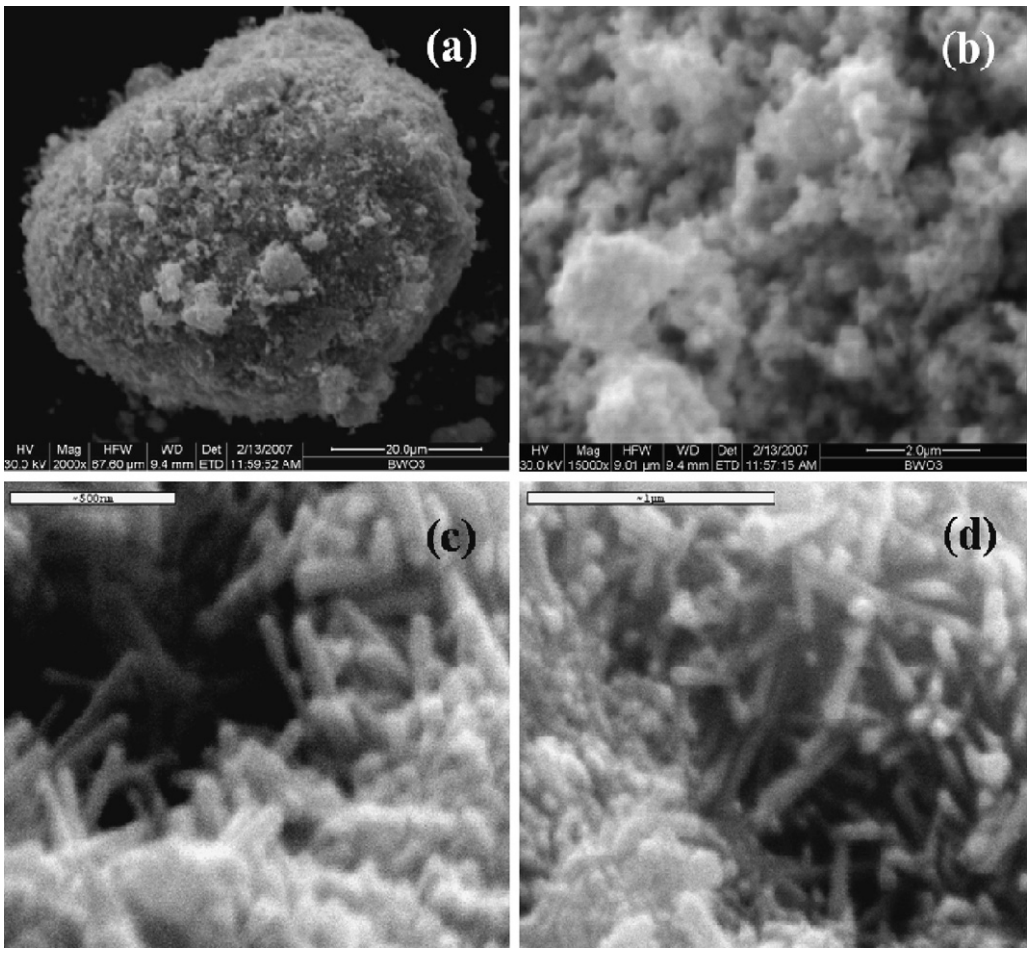

Fig. 3. SEM images of bulk WO_3 (a and b) and WO_3 nanorods (c and d).

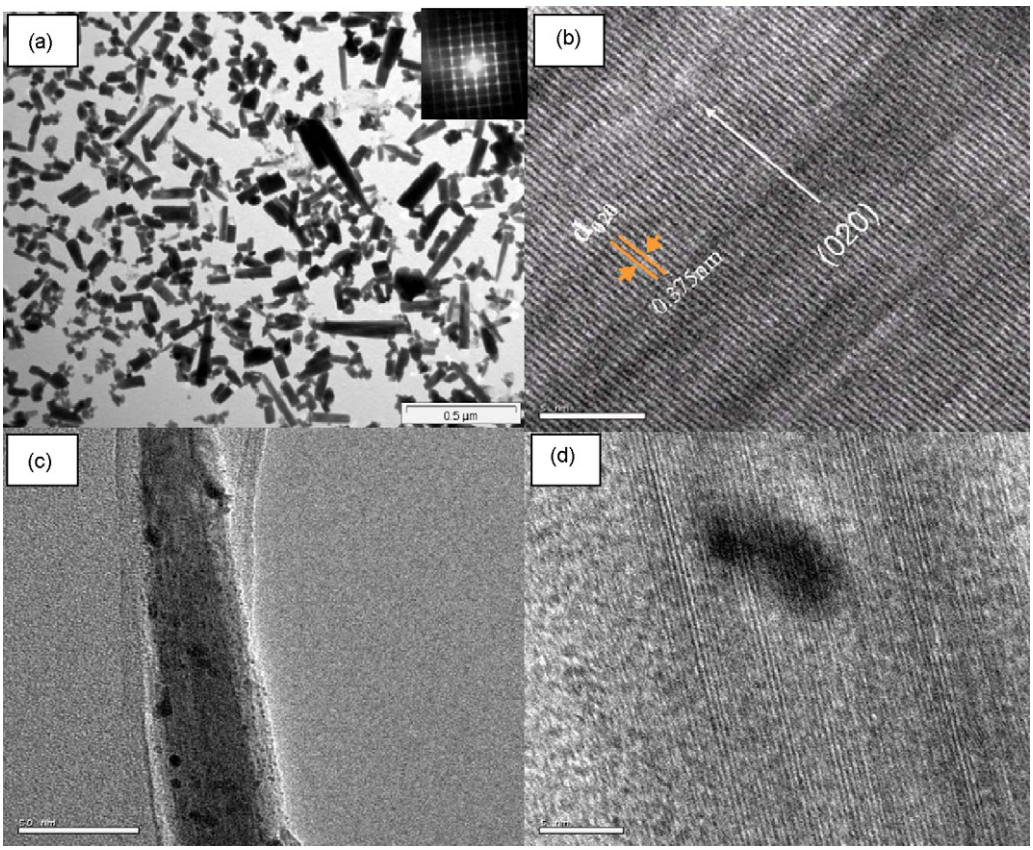

Fig. 4. (a) TEM of WO_3 nanorods (inset: an electron diffraction pattern obtained from the WO_3 nanorod), (b) HRTEM image of a WO_3 nanorod, (c) a low magnification HRTEM image of Pt/WO_3 nanorods, and (d) HRTEM image of a Pt nanoparticle on WO_3 nanorod.

no specific morphology both at low and high magnification. A distribution of nanorods of WO_3 in high yields can be seen from Fig. 3c and d for the as-synthesized tungsten trioxide. This observation is well consistent with TEM observations (Fig. 4a) which also showed rod like morphology. Further, the dimensions of the nanorods calculated from the TEM images vary in the ranges of 130–480 nm and 18–56 nm of length and width, respectively. The inset in Fig. 4a presents a corresponding electron diffraction pattern of WO_3 nanorods, thus indicating the crystallinity of WO_3. The representative high resolution TEM image of a nanorod showing a well resolved lattice is illustrated in Fig. 4b. The lattice fringes calculated are about 0.375 nm and it corresponds to the interplanar spacing of (0 2 0) planes of monoclinic WO_3. This observation agrees with the XRD results (JCPDS card no. 75-2072) and indicates the growth of WO_3 nanorods along (0 2 0) plane. The high resolution TEM images of platinum loaded WO_3 nanorods are shown in Fig. 4c and d. The presence of platinum on the surface of WO_3 nanorods can be seen from Fig. 4c and the size of the Pt nanoparticles calculated is in the range of 4–6 nm. The well resolved lattice fringes of platinum can be evidenced from Fig. 4d. The interplanar spacing calculated from a single platinum nanoparticles is 0.225 nm and this

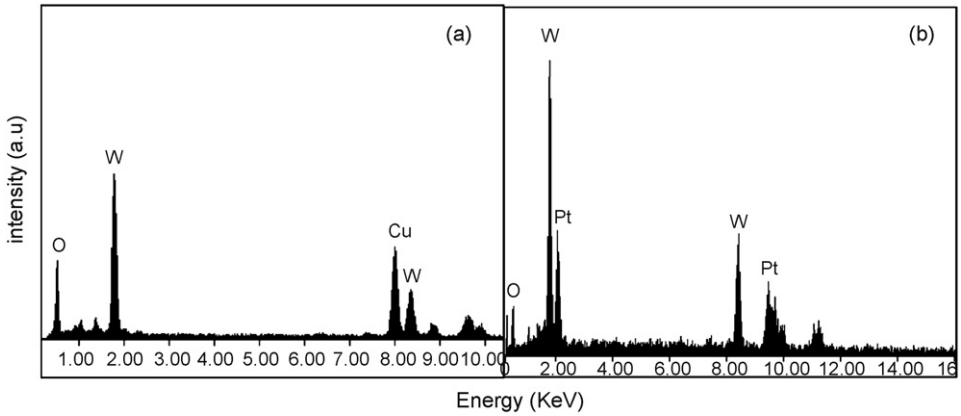

Fig. 5. EDAX analysis of (a) WO_3 nanorods and (b) Pt/WO_3 nanorods.

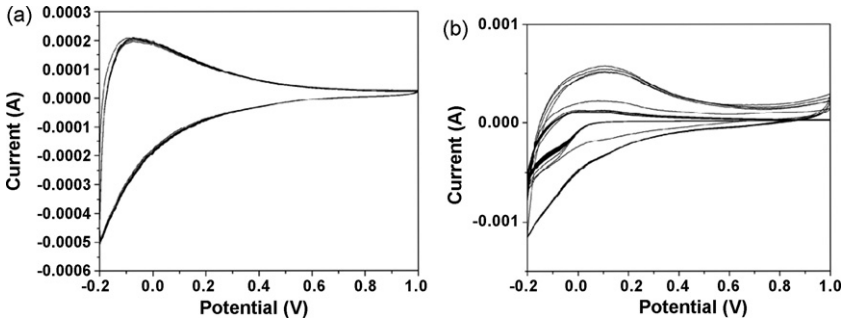

Fig. 6. Cyclic voltammograms of (a) WO_3 nanorods and (b) bulk WO_3 in 1 M H_2SO_4 at a scan rate of 25 mV s^{-1}.

is in agreement with (1 1 1) plane of Pt (JCPDS 04-0802). The EDAX results confirmed the presence of respective constituent elements in WO_3 nanorods and Pt/WO_3 nanorods as shown in the representative EDAX spectra (Fig. 5a and b). The copper signals originate from a copper supporting microgrid.

3.3. Electrocatalytic activity towards methanol oxidation

The electrochemical behavior of WO_3 nanorods and bulk WO_3 were studied in 1 M H_2SO_4. The cyclic voltammograms of WO_3 nanorods (Fig. 6a) and bulk WO_3 (Fig. 6b) showed an anodic peak at −0.07 and +0.1 V, respectively. This peak is attributed to the formation of tungsten bronzes by hydrogen intercalation in the tungsten trioxide. The stability of a catalyst support in acid medium is required for methanol oxidation as the process is carried out in acid medium. This was evaluated by performing uninterrupted cycling of the potential between −0.2 and 1.0 V in 1 M H_2SO_4. For the WO_3 nanorods (Fig. 6a), almost no activity variation was observed even after several cycles indicating its stability in sulfuric acid medium. Whereas for the bulk WO_3, the peak current was observed to decrease showing a poor stability in acid medium. This study reveals that WO_3 nanorods can be better catalytic support for methanol oxidation in comparison to their bulk counterpart.

The electrochemical activity of platinum loaded WO_3 nanorods for methanol oxidation was studied using cyclic voltammetry in the presence of 1 M H_2SO_4 and 1 M CH_3OH (Fig. 7a). The cyclic voltammograms of commercial 20% Pt-Ru/C (J.M.) and Pt loaded on bulk WO_3 are also presented in Fig. 7b and c, respectively. For comparison, the Pt loadings were done at the nominal Pt level in the commercial catalyst, i.e., at 20 wt% for WO_3 nanorods and bulk WO_3. The peak current densities and mass activities due to methanol oxidation are shown in Table 1. The catalyst activities can therefore be ranked in the following order: Pt/WO_3 nanorods > Pt-Ru/C (J.M.) > Pt/bulk WO_3. The reasons for the enhanced activity of platinum loaded WO_3 nanorods may be as follows: (i) unique electrochemical activity of 1D nanostructures, (ii) high utilization of Pt by the nanostructures, (iii) electronic and ionic conductivity of tungsten bronzes and (iv) minimization of CO poisoning by transition metal oxides. The activities of Pt/WO_3 nanorods is approximately six times higher than that of the Pt/bulk WO_3. It appears clearly that the nanostructures of the catalytic support is essential and governs the electroactivity. Methanol oxidation activities of

Table 1
Comparison of electrocatalytic activity of various catalytic systems towards methanol oxidation

Sample	Amount of Pt (μg)	Activity[a] (mA cm^{-2})	Mass activity[b] (mA mg^{-1} Pt)
20% Pt/WO_3 nanorods	50	211	295
20% Pt-Ru/C (J.M.) commercial	50	192	268
20% Pt/bulk WO_3	50	35	49

[a] Peak current density at 0.76 V.
[b] Activity per mg Pt.

Pt loaded WO_3 nanorods are slightly higher or comparable to that of the commercial catalyst. This shows that replacement of the noble metal Ru in the commercial catalyst is possible with WO_3 nanorods as its properties allow to play the role of Ru as well as carbon support. All these facts demonstrate that WO_3 nanorods are better supports for platinum than bulk WO_3 and carbon and hence they constitute a better catalytic system for methanol oxidation.

To show the electrochemical stability of the three catalysts for methanol oxidation, chronoamperometric experiments were carried out. Fig. 8 shows the current–time plot for the three catalytic systems in 1 M H_2SO_4 and 1 M CH_3OH at 0.6 V. Fig. 8a

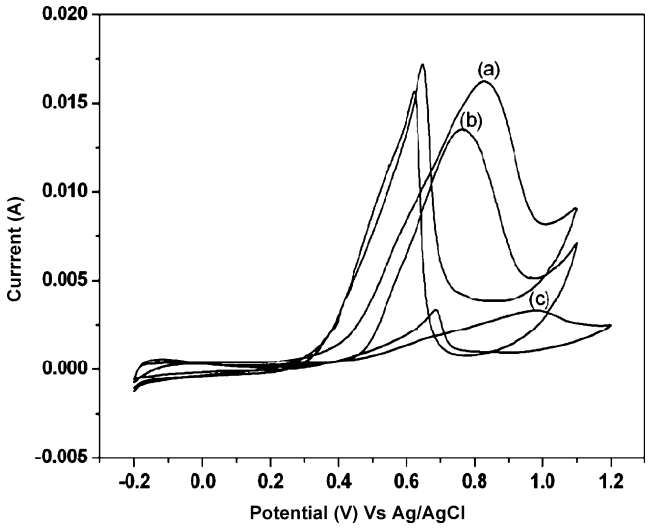

Fig. 7. Cyclic voltammograms of (a) 20% Pt/WO_3 nanorods, (b) 20% Pt-Ru/C (J.M.), and (c) 20% Pt/bulk WO_3 in 1 M CH_3OH–1 M H_2SO_4 at a scan rate of 25 mV s^{-1}.

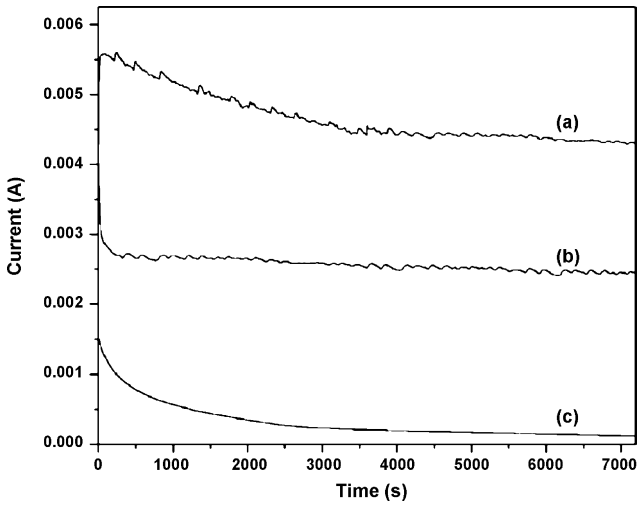

Fig. 8. Chronoamperometric response of (a) 20% Pt/WO_3 nanorods, (b) 20% Pt-Ru/C (J.M), and (c) 20% Pt/bulk WO_3 at 0.6 V.

shows the chronoamperometric response of the Pt loaded WO_3 nanorods. The electrode shows higher initial activity when compared to the other two catalytic systems. It shows a gradual decay in the current till 4000 s and remained stable afterwards. The commercial Pt-Ru/C (J.M.) (Fig. 8b) constitutes a stable catalytic system but at any point of time, the activity of the system is lower than the Pt loaded WO_3 nanorod system. This shows the better electrocatalytic performance of nanorod supported system than the commercial Pt-Ru/C (J.M.) system. The performance of Pt loaded on bulk WO_3 (Fig. 8c) was found to be poor compared to the commercial Pt-Ru/C (J.M.) and Pt/WO_3 nanorods in terms of activity and stability. The initial activity of the Pt/bulk WO_3 is lower than the commercial Pt-Ru/C (J.M.) and Pt/WO_3 nanorods and the current decays throughout the time of the experiment. The final current value at 7200 s is higher for Pt loaded WO_3 nanorods than the other two systems. The test shows that the Pt loaded on WO_3 nanorod system has the best electrocatalytic performance among all the studied electrocatalysts.

4. Conclusion

In summary, a simple and easy method is adopted to fabricate WO_3 nanorods. The sizes of the nanorods range in 130–480 nm in length and 18–56 nm in width. The adopted synthetic procedure opens up a newer route for the synthesis of a variety of transition metal oxide nanorods by choosing suitable precursor compounds, which is under progress. Methanol oxidation was carried out using platinum loaded on these WO_3 nanorods. The comparable methanol oxidation activity of platinum loaded WO_3 nanorods with that of the commercial 20% Pt-Ru/C catalyst suggests that the noble metal Ru can be replaced with low cost metal oxide nanorods. However, role of the nanoarchitectures of support on the observed activity is still to be understood fully.

References

[1] S. Wasmus, A. Kuver, Electrochim. Acta 45 (2000) 4319.
[2] X. Ren, P. Zelenay, A. Thomas, J. Davey, S. Gottesfeld, J. Power Sources 86 (2000) 111.
[3] X. Ren, M.S. Wilson, S. Gottesfeld, J. Electrochem. Soc. 143 (1996) L12.
[4] D. Kim, E.A. Cho, S.A. Hong, I.H. Oh, H.Y. Ha, J. Power Sources 130 (2004) 172.
[5] E. Reddington, A. Sapienza, B. Gurau, R. Viswanathan, S. Sarangapani, E.S. Smotkin, T.E. Mallouk, Science 280 (1998) 1735.
[6] B.D. McNicol, D.A.J. Rand, K.R. Williams, J. Power Sources 83 (1999) 15.
[7] A.K. Shukla, P.A. Christensen, A.J. Dickinson, H. Hamnett, L. Carrette, K.A. Frisdich, U. Stimming, Chem. Phys. Chem. 1 (2000) 162.
[8] A.S. Aricò, V. Baglio, E. Modica, A. Di Blasi, V. Antonucci, Electrochem. Commun. 6 (2004) 164.
[9] A. Hamnett, Catal. Today 38 (1997) 445.
[10] W. Vielstich, J. Brazil. Chem. Soc. 14 (2003) 503.
[11] M.B. de Oliveira, L.P.R. Profeti, P. Olivi, Electrochem. Commun. 7 (2005) 703.
[12] N. Marcovic, H.A. Gasteiger, P.N. Ross, X. Jiang, I. Villegas, M.J. Weaver, Electrochim. Acta 40 (1995) 91.
[13] G.T. Burstein, C.T. Barnett, A.R. Kucernak, K.R. Williams, Catal. Today 38 (1997) 425.
[14] T. Okada, N. Arimura, C. Ono, M. Yuasa, Electrochim. Acta 51 (2005) 1130.
[15] J.W. Guo, T.S. Zhao, J. Prabhuram, R. Chen, C.W. Wong, Electrochim. Acta 51 (2005) 754.
[16] J. Guo, G. Sun, Q. Wang, G. Wang, Z. Zhou, S. Tang, L. Jiang, B. Zhou, Q. Xin, Carbon 44 (2006) 152.
[17] L. Jiang, G. Sun, S. Sun, J. Liu, S. Tang, H. Li, B. Zhou, Q. Xin, Electrochim. Acta 50 (2005) 5384.
[18] B.N. Grgur, N.M. Markovic, P.N. Ross, Electrochim. Acta 43 (1998) 3631.
[19] H.M. Villullas, F.I. Mattos-Costa, L.O.S. Bulhoes, J. Phys. Chem. B 108 (2004) 12898.
[20] H.A. Gasteiger, N. Markovic, P.N. Ross, E.J. Cairns, J. Phys. Chem. 97 (1993) 12020.
[21] M.M.P. Janssen, J. Moolhuysen, J. Catal. 46 (1977) 289.
[22] M.M.P. Janssen, J. Moolhuysen, Electrochim. Acta 21 (1976) 869.
[23] H.A. Kozlowska, B. MacDougall, B.E. Conway, J. Electrochem. Soc. 120 (1973) 756.
[24] J. Xu, K. Hua, G. Sun, C. Wang, X. Lv, Y. Wang, Electrochem. Commun. 8 (2006) 982.
[25] K. Lasch, L. Jorissen, J. Garche, J. Power Sources 84 (1999) 225.
[26] S.H. Baeck, T.F. Jaramillo, G.D. Stucky, E.W. McFarland, Nano Lett. 2 (2002) 831.
[27] K.W. Park, K.S. Ahn, Y.C. Nah, J.H. Choi, Y.E. Sung, J. Phys. Chem. B 107 (2003) 4352.
[28] P.K. Shen, A.C.C. Tseung, J. Electrochem. Soc. 141 (1994) 3082.
[29] P.K. Shen, K.Y. Chen, A.C.C. Tseung, J. Chem. Soc., Faraday Trans. 90 (1994) 3089.
[30] A.K. Shukla, M.K. Ravikumar, A.S. Arico, G. Candiano, V. Antonucci, N. Giordano, A. Hamnett, J. Appl. Electrochem. 25 (1995) 528.
[31] L. Su, L. Zhang, J. Fang, M. Xu, Z. Lu, Sol. Energy Mater. Sol. Cells 58 (1999) 133.
[32] M. Umeda, H. Ojima, M. Mohamedi, I. Uchida, J. Power Sources 136 (2004) 10.
[33] L.X. Yang, C. Bock, B. McDougall, J. Park, J. Appl. Electrochem. 34 (2004) 427.
[34] P.J. Barczuk, H. Tsuchiya, J.M. Macak, P. Schmuki, D. Szymanska, O. Makowski, K. Miecznikowski, P.J. Kulesza, Electrochem. Solid-State Lett. 9 (2006) E13.
[35] B. Rajesh, K.R. Thampi, J.M. Bonard, B. Viswanathan, J. Phys. Chem. B 107 (2003) 2701.
[36] V. Raghuveer, B. Viswanathan, J. Power. Sources 144 (2005) 1.
[37] S. Jayaraman, T.F. Jaramillo, S.H. Baeck, E.W. McFarland, J. Phys. Chem. B 109 (2005) 22958.
[38] R. Ganesan, J.S. Lee, J. Power Sources 157 (2006) 217.
[39] R. Narayanan, M.A. El-Sayed, J. Am. Chem. Soc. 126 (2004) 7194.
[40] R. Narayanan, M.A. El-Sayed, Nano Lett. 4 (2004) 1343.

[41] G.R. Patzke, F. Krumeich, R. Nesper, Angew. Chem. Int. Ed. 41 (2002) 2446.
[42] S.H. Yu, B. Liu, M.S. Mo, J.H. Huang, X.M. Liu, Y.T. Qian, Adv. Funct. Mater. 13 (2003) 639.
[43] J. Liu, Y. Zhao, Z. Zhang, J. Phys.: Condens. Matter (2003) L453.
[44] H. Zhang, M. Feng, F. Liu, L. Liu, H. Chen, H. Gao, J. Li, Chem. Phys. Lett. 389 (2004) 337.
[45] Y.Q. Zhu, W. Hu, W.K. Hsu, M. Terrones, N. Grobert, J.P. Hare, H.W. Kroto, D.R.M. Walton, H. Terrones, Chem. Phys. Lett. 309 (1999) 327.
[46] X.W. Lou, H.C. Zeng, Inorg. Chem. 42 (2003) 6169.
[47] S.V. Pol, V.G. Pol, G.A. Seisenbaeva, L.A. Solovyov, A. Gedanken, Inorg. Chem. 44 (2005) 9938.
[48] M. Gillet, R. Delamare, E. Gillet, J. Crystal Growth 279 (2005) 93.
[49] A. Chemseddine, C. Sanchez, J. Livage, P. Launay, M. Fournier, Inorg. Chem. 23 (1984) 2609.
[50] C. Santato, M. Odziemkowski, M. Ulmann, J. Augustynski, J. Am. Chem. Soc. 123 (2001) 10639.
[51] A. Cremonesi, D. Bersani, P.P. Lottici, Y. Djaoued, P.V. Ashrit, J. Non-Cryst. Solids 345–346 (2004) 500.
[52] B. Palys, M.I. Borzenko, G.A. Tsirlina, K. Jackowska, E.V. Timofeeva, O.A. Petrii, Electrochim. Acta 50 (2005) 1693.